

## Imaging of surface acoustic waves

C. Bodefeld, F. Beil, H.-J. Kutschera, M. Streibl, Achim Wixforth

### Angaben zur Veröffentlichung / Publication details:

Bodefeld, C., F. Beil, H.-J. Kutschera, M. Streibl, and Achim Wixforth. 2001. "Imaging of surface acoustic waves." In *IEEE Ultrasonics Symposium Proceedings: An International Symposium, 7 - 10 October 2001, Atlanta, GA, USA*, 145–48. Piscataway, NJ: IEEE.  
<https://doi.org/10.1109/ultsym.2001.991596>.

### Nutzungsbedingungen / Terms of use:

licgercopyright

Dieses Dokument wird unter folgenden Bedingungen zur Verfügung gestellt: / This document is made available under these conditions:

**Deutsches Urheberrecht**

Weitere Informationen finden Sie unter: / For more information see:

<https://www.uni-augsburg.de/de/organisation/bibliothek/publizieren-zitieren-archivieren/publiz/>



# Imaging of Surface Acoustic Waves

C. Bödefeld, F. Beil, H.-J. Kutschera, M. Streibl, and A. Wixforth

Sektion Physik der Ludwig Maximilians Universität and CeNS, Geschwister-Scholl-Platz 1, 80539 München, Germany

**Abstract**— A new method to optically examine surface acoustic wave (SAW) propagation on a semiconductor chip is presented. This visualization method is based on the influence of a SAW on the optical properties of a piezoelectric semiconductor. There are two interaction mechanisms between the SAW and photo generated carriers that allow to correlate the photoluminescence (PL) to the power of the SAW: First exciton dissociation leads to a reduction of the PL and second trapped charge carriers can be released leading to an enhancement of the PL. In the experiment we use a gated and intensified CCD camera to directly record light coming from the sample. With our setup we are able to display the temporal and spatial distribution of SAW fields with a resolution of 300 ps and 1  $\mu$ m respectively.

## I. INTRODUCTION

Surface acoustic waves (SAW) are of tremendous importance in the field of radio frequency signal processing. Sophisticated transducer design and material engineering led to the emerging of novel devices of most any desired functionality. This is due to the fact that the theory of elastic wave propagation as well as the understanding of the design and layout of transducing devices are rather advanced, these days. However, sometimes it is still desirable to actually ‘watch’ a device under operating conditions if one is interested in spurious signals, standing wave patterns or simply energy flow. The visualization of a propagating SAW on the surface of an appropriate substrate has hence been treated by many different approaches. Stroboscopic electron beam[1, 2], X-Ray topography[3] as well as probe techniques such as force[4] and capacitive[5] probing have been employed.

Here, we would like to discuss a novel visualization technique being well suited to map out especially the piezoelectric field distributions in a traveling SAW. For this purpose, we describe the interaction between a SAW and photogenerated carriers in a semiconductor layered system on the one hand and secondly,

the influence of a piezo-active SAW on carriers being trapped in shallow states in the semiconductor. To make our experiments more transparent, the presented results have all been taken at low temperatures ( $T = 4$  K).

## II. INTERACTION OF SAW WITH SEMICONDUCTOR SAMPLES

To visualize the piezoelectric field distribution in a traveling SAW, we first have to consider possible interaction mechanisms between those fields and any observable in the system: The first is known as acoustical quenching of semiconductor photoluminescence (PL). Here, the strong lateral piezoelectric fields in a SAW can field-ionize photogenerated electron-hole complexes and hence spatially separate the fragments [6, 7, 8]. This in turn strongly reduces the probability for radiative recombination and finally leads to a quenching of the PL. A sketch of the mechanism is shown in the inset of fig. 1, indicating the spatial separation of the photogenerated charges. Hence, if one is able to homogeneously illuminate such a semiconductor sample, and to observe the PL coming from it, a propagating piezoelectric SAW shows up as a ‘dark spot’ in the PL photograph. This is shown in fig. 1, where we show a snapshot of a propagating SAW on a GaAs based quantum well sample, using a technique as described below.

Second, impurity and trap related recombination processes can be used to visualize the SAW as they are also modified by the electric fields, deformation potential and heating associated with the SAW[9]. The SAW increases trap emission rates and leads therefore to a increased number of free carriers, which are then able to radiatively recombine. A sample containing a large number of trapped charges that can be released by a SAW should then exhibit ‘bright spots’ at the sites of large trap concentration.

Of course, both interaction mechanisms are opposed to each other in terms of their effects. It depends on the sample which interaction plays the major role. In the following, we present experiments for both cases. As one will see in each case the main effect dominates in such a way, that a qualitative statement about the SAW power is possible.

It turns out that our method is exceptionally well suited to examine the SAW fields of sophisticated IDT structures as it does not use any probe waves or complicated setups and is therefore not restricted to special directions, frequencies or structures.

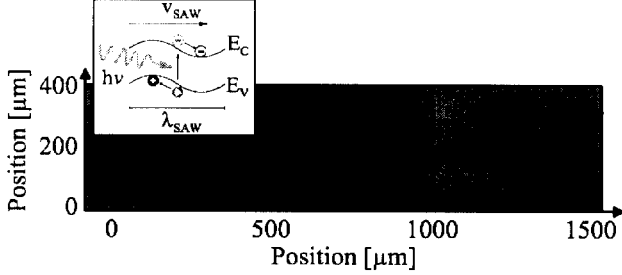


Fig. 1. Image of the impact of a SAW on a semiconductor heterostructure. We show the change in photoluminescence (PL) intensity caused by a SAW moving from left to right. The integration time for this picture was  $t_{int} = 10$  ns. The dark area corresponds to high SAW power due to quenching of the PL. Note the slightly brighter area right to the intensity minimum. It is believed that here carriers in traps are activated by the SAW and recombine. A sketch of the mechanism of PL quenching is shown in the inset. An exciton is formed by absorbing a photon ( $h\nu$ ). This exciton can be split up by the strong electric fields of the SAW as indicated by the conduction and valence band modulation. The spatially separated carriers are trapped in the moving lateral potential wells, being  $\lambda_{SAW}/2$  apart from each other. Hence, recombination is strongly suppressed.

### III. EXPERIMENTAL SETUP

Our samples are mounted in an optical cryostat, providing temperatures as low as  $T = 4$  K. It can be illuminated externally by a pulsed laser and SAW can be excited using different interdigitated transducer geometries. The whole experiment is triggered by a pulse generator, whose repetition rate is set to 100 kHz. The same pulse generator triggers the laser, the SAW, and the infrared detector, consisting of an intensified gated CCD.

To illuminate the sample and detect the PL light a standard confocal setup with variable microscope objectives ranging from 5x to 80x was used. To reduce any reflected and stray laser light, which could damage the detector, an edge filter blocking the light below 780 nm is utilized. A laser diode illuminates the sample with above bandgap radiation at  $\lambda = 680$  nm. The photoluminescence is then detected by an intensified CCD, providing a time resolution of  $t_{min} = 300$  ps and being sensitive up to a wave length of  $\lambda_{max} = 900$  nm.

To optically pump the semiconductor, the laser is turned on only for a time of  $t_{laser} = 50$  ns. Single PL

images are taken at the repetition rate of the whole setup, i.e. 100 kHz. They are co-added in the CCD to a so called frame, which is read out by a computer every 20 ms. To enhance the S/N ratio, a software averages the frames to a single picture. In the presented experiments 255 frames were integrated, which translates with an opening time of  $t_{int} = 10$  ns to a total integration time of  $255 \text{ Frames/Picture} \times 20 \text{ ms/Frame} \times 10 \text{ ns} / 10 \mu\text{s} = 5.1 \text{ ms/Picture}$ .

The pictures have been taken with different integration times ranging from  $t_{int} = 300$  ps to 25 ns at a time when the laser is on. The timing sequence between laser, SAW, and detection gate then allows for a stroboscopic imaging of the PL and the influence of the SAW on it.

## IV. EXPERIMENTAL RESULTS

### A. Images of plain transducers

First, we want to present an experiment employing the quenching of the PL as the main interaction. As described above, a SAW moving through the observed area reduces the PL. In fig. 1 an image with an integration time of  $t_{int} = 10$  ns has been taken 325 ns after the RF-pulse of frequency  $f = 470$  MHz, power  $P = 34$  dBm and  $t = 40$  ns duration had been applied. The sample is a GaAs/  $\text{In}_{0.15}\text{Ga}_{0.85}\text{As}$  heterostructure with a quantum well of 100 Å thickness. The quantum well has been etched on all areas surrounding the SAW path to reduce stray light. Without SAW, the sample appears uniformly bright, as the uniform illumination creates electron hole pairs which radiatively recombine by emitting PL light. Once a SAW is present, however, the piezoelectric fields quench the PL on the respective area of the sample. This is observed as a dark spot, which is clearly seen in the figure, where we show a snapshot of a SAW, which has traveled approximately 950 μm.

Looking more closely into the picture of the SAW, other features appear: A curvature of the wave front and a small area of increased light intensity right in front of the main wave packet. Whereas the first feature can be simply explained with simulations, the second is probably due to the second interaction mechanism mentioned before: Acoustically driven recombination of trapped carriers. Here, the emission rate of the traps is modified by the SAW[9]. However, it is not yet clear why this effect and hence the bright area shows up some 100 μm in front of the wave.

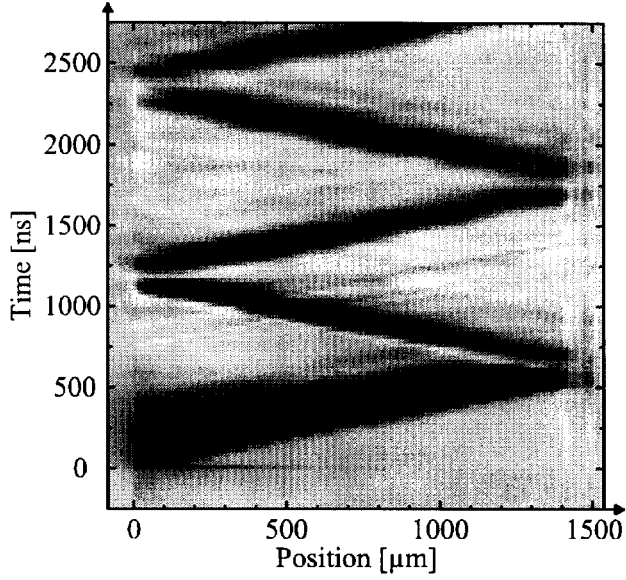


Fig. 2. Multiple reflections of a single SAW pulse depicted as a time series of cross sections along the SAW path. The change in PL intensity of a GaAs/In<sub>0.15</sub>Ga<sub>0.85</sub>As heterostructure has been plotted against time (up) and position on the sample (right). Black corresponds to reduced, white to increased PL intensity. The central part of the SAW path in fig. 1 was integrated to get a curve for each time respectively. A SAW is launched at a time  $t_0 = 0$  ns. Up to 4 reflections can be seen together with secondary waves. Again, recombination is enhanced right in front of the wave packet. This is probably due to activation of trapped carriers.

### B. Time series

The imaging technique can now be used to visualize the temporal evolution of a propagating SAW. For this purpose the central part of fig. 1 has been integrated normal to the propagation direction. These curves are then displayed for consecutive times in fig. 2. Interesting features can be identified: Not only multiple echos are reflected from the IDTs. Furthermore one can see that lots of different waves with smaller amplitude are traveling across the sample. These are probably due to reflections at the chip edges or other structures. Also, the well known ‘triple transit echo’ seems to be split up into two wave packets. And last but not least increased light intensity as described in fig. 1 can be seen right in front of the wave.

### C. Images of complex wave fields

Our visualization method can also be used to study the wave fields of complex IDT structures. As an example the SAW fields of a focusing transducers are imaged via the second interaction mechanism

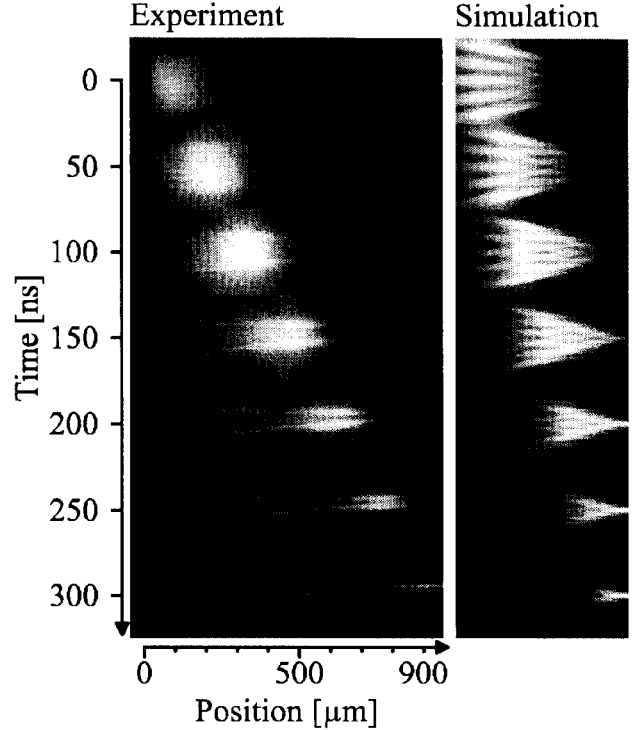


Fig. 3. Visualization of the piezoelectric fields corresponding to a SAW excited by a complex focusing transducer (left). The right panel shows the corresponding results of our simulation procedure as explained in the text (not to scale). To visualize the SAW fields, in this figure the timing sequence of the experiment has been chosen such that the SAW activated emission of trapped carriers gives the recorded signal. Note the fine structure in the lateral field distribution which can be nicely reproduced by the calculation. It turns out that this fine structure arises from interference of waves coming from different parts of the transducer.

and directly compared to the prediction of a simple model[10]. In this model, the SAW field is calculated by a numerical method based on a Huygens-type construction. Taking into account the runtime and the slowness curves of the material, also pulsed SAW can be simulated.

Nearly perfect agreement between the simulation and the experiment is achieved, as can be seen in fig. 3. The sample shown here has been deliberately treated to increase the number of surface states acting as traps for photogenerated carriers. This results in a very bright SAW induced PL from the trapped charges.

The experiment is as follows: The sample is again illuminated with above band gap radiation. The surface states and other traps hence are occupied. After the laser has been turned off, a SAW is launched. At a given time the detector is switched on, recording

light being emitted long time after the illumination has been turned off. This time has been extended up to 20  $\mu$ s without significant differences in the emitted light intensity. This means carriers are efficiently stored in traps and surface states but are released by the SAW allowing us to photograph the SAW power distribution.

The left part of fig. 3 shows a time series of the PL induced by a focused SAW. An interference pattern resulting from waves coming from different parts of the focusing transducer shows up as fine structure in the PL images. These interference patterns are easily understood given the actual layout of the IDT: Instead of defining curved IDT fingers, they are actually piecewise linear, giving rise to the emission of plane wave fronts from these pieces which the interfere in the observed fashion. This fine structure together with the simulations shown in the right panel impressively demonstrate the resolution of our experiments.

Detailed analysis of the experiment shown in fig. 3 suggests that in this experiment only parts of the IDT segments are active. The outermost segments of the curved transducer are too much off axis in terms of coupling coefficient to effectively excite a SAW. For GaAs, we thus can conclude that a maximum tilt angle between 10 and 13 degrees off the [011] direction is allowed.

## V. CONCLUSIONS

In summary, we have demonstrated a novel visualization method for the piezoelectric fields traveling with a SAW. The method is based on the interaction of a SAW with photogenerated charges in semiconductors. Either SAW activated emission from trapped charges or quenching of the PL from photogenerated electron-hole pairs can result in images of the potential distribution in the SAW. A spatial and time resolved imaging system enables us to directly take live images of SAW devices in operation.

## VI. ACKNOWLEDGMENTS

The authors gratefully acknowledge fruitful discussions with W. Ruile A. O. Govorov, and J. P. Kotthaus, H. Lipsanen and his group for providing us with samples and financial support by the Deutsche Forschungsgemeinschaft (SFB 348).

## REFERENCES

- [1] G. Eberharter and H. P. Feuerbaum, *Scanning-electron-microscope observations of propagating acoustic waves in surface acoustic wave devices*, Appl. Phys. Lett. **37**, 698 (1980).
- [2] R. Veith, G. Eberharter, H. P. Feuerbaum, and U. Knauer, *Visualization of SAW propagation with the scanning electron microscope*, Proc. 1980 IEEE Ultrasonics Symposium, vol. 2, pp. 1089, vol. 1, pp. 348, 1980.
- [3] W. Sauer, M. Streibl, T. H. Metzger, A. G. C. Haubrich, S. Manus, A. Wixforth, J. Peisl, A. Mazuelas, J. Hartwig and J. Baruchel, *X-ray imaging and diffraction from surface phonons on GaAs*, Appl. Phys. Lett. **75**, 1709 (1999).
- [4] T. Hesjedal, E. Chilla, and H.J. Frohlich, *High resolution visualization of acoustic wave fields within surface acoustic wave devices*, Appl. Phys. Lett. **70**, 1372 (1997).
- [5] B. A. Richardson and G. S. Kino, *Probing of elastic surface waves in piezoelectric media*, Appl. Phys. Lett. **16**, 82 (1970).
- [6] C. Rocke, S. Zimmermann, A. Wixforth, and J. P. Kotthaus, *Acoustically Driven Storage of Light in a Quantum Well*, Phys. Rev. Lett. **78**, 4099 (1997).
- [7] K. S. Zhuravlev, D. V. Petrov, Yu. B. Bolkhovityanov, and N. S. Rudaja, *Effect of surface acoustic waves on low temperature photoluminescence of GaAs*, Appl. Phys. Lett. **70**, 3389 (1997).
- [8] P. V. Santos, M. Ramsteiner, and F. Jungnickel, *Spatially resolved photoluminescence in GaAs surface acoustic wave structures*, Appl. Phys. Lett. **72**, 2099 (1998).
- [9] D. Janes and M. J. Hoskins, *Trap Emission Rates in GaAs in the Presence of Surface Acoustic Waves*, J. Appl. Phys. **67**, 6315 (1990).
- [10] M. Streibl, H.-J. Kutschera, W. Sauer, and A. Wixforth, *Numerical and Experimental Analysis of Complex Surface Acoustic Wave Fields*, Proc. 2000 IEEE Ultrasonics Symposium, vol.1, p.205-208, 2001.